Photosensitizer–Gold Nanorod Composite for Targeted Multimodal Therapy

Jian Wang, Mingxu You, Guizhi Zhu, Mohammed Ibrahim Shukoor, Zhuo Chen, Zilong Zhao, Meghan B. Altman, Quan Yuan, Zhi Zhu, Yan Chen, Cheng Zhi Huang, and Weihong Tan**

In this work, a DNA inter-strand replacement strategy for therapeutic activity is successfully designed for multimodal therapy. In this multimodal therapy, chlorin e6 (Ce6) photosensitizer molecules are used for photodynamic therapy (PDT), while aptamer-AuNRs, are used for selective binding to target cancer cells and for photothermal therapy (PTT) with near infrared laser irradiation. Aptamer Sgc8, which specifically targets leukemia T cells, is conjugated to an AuNR by a thiol-Au covalent bond and then hybridized with a Ce6-labeled photosensitizer/reporter to form a DNA double helix. When target cancer cells are absent, Ce6 is quenched and shows no PDT effect. However, when target cancer cells are present, the aptamer changes structure to release Ce6 to produce singlet oxygen for PDT upon light irradiation. Importantly, by combining photosensitizer and photothermal agents, PTT/PDT dual therapy supplies a more effective therapeutic outcome than either therapeutic modality alone.

1. Introduction

Over the last few decades, clinicians have made increasing use of anticancer drugs to treat a wide variety of deadly cancers,[1] for example, leukemia,[2] lung cancer,[3] breast cancer[4] and prostate cancer.[5] However, most anticancer drugs in clinical use are limited by their general toxicity to proliferating cells, including some normal cells,[6] leading to the unwanted side effects. Furthermore, most cancers are solid tumors, which can be cured by ablation. However, leukemia, a type of blood or bone marrow cancer, is difficult to target and kill. Since bone marrow transplantation is often

Dr. J. Wang, Dr. M. You, G. Zhu, Dr. M. I. Shukoor, Dr. M. B. Altman, Prof. W. Tan
Center for Research at the Bio/Nano Interface
Department of Chemistry and Shands Cancer Center
University of Florida Genetics Institute
University of Florida
Gainesville, FL 32611-7200, USA
E-mail: tan@chem.ufl.edu

Dr. J. Wang, Prof. C. Z. Huang
Ministry of Education Key Laboratory on Luminescence and Real-Time Analysis
College of Pharmaceutical Sciences
Southwest University
Chongqing, 400715, China
E-mail: chengzhi@swu.edu.cn

Prof. Z. Chen, Dr. Z. Zhao, Dr. Q. Yuan, Dr. Z. Zhu, Dr. Y. Chen, Prof. W. Tan
Molecular Sciences and Biomedicine Laboratory
State Key Laboratory for Chemo/Biosensing and Chemometrics
College of Biology and College of Chemistry and Chemical Engineering
Collaborative Innovation Center for Chemistry and Molecular Medicine
Hunan University
Changsha 410082, China

DOI: 10.1002/smll.201202155

NANO MICRO small

required for these patients, a targeted and effective therapy that could specifically kill leukemia cells, while leaving normal cells unharmed, would be highly desirable.

These issues can be addressed by the development of aptamer probes that can specifically recognize their target cell cognate.[7] Briefly, aptamers are single-stranded DNA or RNA (ssDNA or ssRNA), which can bind a wide range of targets, including small molecules,[8,9] proteins[10,11] and intact cells[12,13] with high affinities and specificities.[14] As recognition elements, aptamers possess many significant advantages over antibodies, including flexible design, synthetic accessibility, easy modification, chemical stability, reversible denaturation and rapid tissue penetration,[14] which make aptamers promising probes to elucidate the molecular foundation of diseases, particularly cancers.[15]

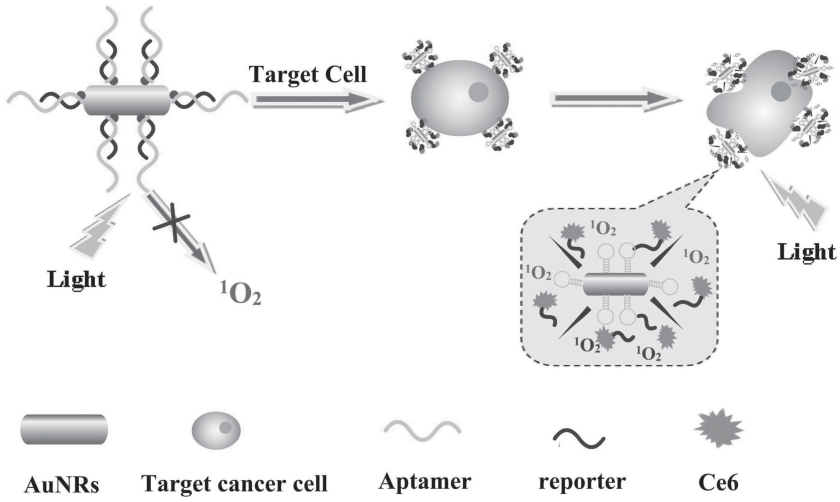

Scheme 1. Schematic diagram of aptamer-conjugated AuNR-Ce6 complex for targeted cancer therapy.

As one method of functionalizing such aptamer probes, gold nanorods (AuNRs), have been studied extensively.[12,16–18] The strong surface plasmon absorption band of AuNRs in the near-infrared (NIR) region can be easily tuned by adjusting the aspect ratio. Their large surface electric field and absorption cross section allow AuNRs to efficiently convert the absorbed radiation into heat,[19] which kills the targeted cells.[20] Thus, AuNRs are efficient energy quenchers and hyperthermia agents for photothermal therapy (PTT),[12,21,22] which utilizes electromagnetic radiation, most often in the NIR region.

In addition, aptamer-photosensitizer conjugates have been used for photodynamic therapy (PDT) with a high degree of selectivity.[23,24] In PDT, reactive oxygen species (ROS) are generated when photosensitizers are exposed to light in a specific wavelength band. Photosensitizers currently used in PDT are usually nontoxic to cells before light irradiation ("off" state). When exposed to light, these sensitizers can actively generate ROS, including singlet oxygen, to kill the tumor ("on" state).[12,21,23] However, with limited tumor-selectivity, the activation of singlet oxygen by photosensitizers can result in nonspecific damage to normal tissues upon exposure to light. Even though many efficient photosensitizers have been developed with the ability to kill cancer cells,[21] the lack of target specificity results in indiscriminate release of singlet oxygen, thereby causing damage to non-target cells. To address the issue of controllable target specificity, Chlorin e6 (Ce6), a second-generation and easily modifiable photosensitizer, was employed in our group, to enhance PDT selectivity in targeting cancer cells by using aptamer-Ce6 conjugates. Target-specific PDT was achieved by manipulating the quenching and recovery of photosensitizer fluorescence emission, which was, in turn, tuned by controlling the distance between the quencher and photosensitizer.[23]

The development of multimodal therapy, such as PDT and PTT, is currently being pursued. Both the Choi[21] and Yeh[22] groups have developed multimodal therapy using AuNRs and photosensitizers for photothermal and photodynamic killing of tumors with enhanced efficiency compared with either PTT or PDT alone. However, some specificity problems have strongly impeded the use of these systems in clinical applications. First, the photosensitizer was electrostatically attached to the gold surface, making it difficult to control the release. Furthermore, the therapy was based on a passive targeting mechanism with low selectivity for targeting cancer cells.[21,22]

To solve this problem, we have designed a targeted cancer therapy by using one intrachain aptamer switch probe,[12] which has greatly enhanced the specificity. In this work, we propose another switchable aptamer-based photosensitizer-AuNR platform for targeted multimodal therapy, using leukemia as a model cancer for proof of concept, to provide a highly specific and enhanced therapeutic outcome.

2. Results and Discussion

2.1. Design for Multimodal Cancer Therapy

In this multimodal therapy design (**Scheme 1**), both PTT and PDT are employed to kill cancer cells. First of all, a target-specific aptamer is conjugated with AuNR by a thiol-Au covalent bond and then hybridized with a Ce6-labeled photosensitizer/reporter to form DNA double strands. In this instance, the Ce6 is non-phototoxic based on the quenching effect of the gold surface adsorption.[12,21,22] However, upon binding the target cancer cells, the aptamer forms a molecular beacon structure[25] and releases the reporter strand. After release, Ce6 becomes phototoxic and can be used for PDT to kill target cancer cells. Furthermore, aptamer-AuNR conjugates can be further employed for PTT with irradiation by a NIR laser. Besides, AuNRs are also helpful for the delivery and activation of photosensitizer molecules. It is expected that this multimodal PDT/PTT strategy can more effectively kill disease cells than either therapy alone.

2.2. Preparation and Characterization of AuNRs

AuNRs were prepared by the seed-mediated method[26] so that the longitudinal plasmon resonance absorption (LPRA) band was located at 750 nm with an aspect ratio of 3.3 (Figure S1, Supporting Information). The overlap of the AuNRs' LPRA band with the fluorescence emission of Ce6 (Figure S2, Supporting Information) is the basis for preventing the release of singlet oxygen, thus sufficiently reducing the background and avoiding nonspecific photodestruction. It is noteworthy that a single AuNR can carry multiple Ce6-conjugates to the cell surface,[27,28] resulting in a high local concentration of the photosensitizers for more efficient killing of the target cells with fewer side effects. In addition, AuNRs with photothermal capability can convert laser photonic energy into heat, and the resulting heat energy can be used for PTT, as well as gradual release of the prehybridized sequence of Ce6-reporter,[29] to enhance the therapeutic efficacy.[20]

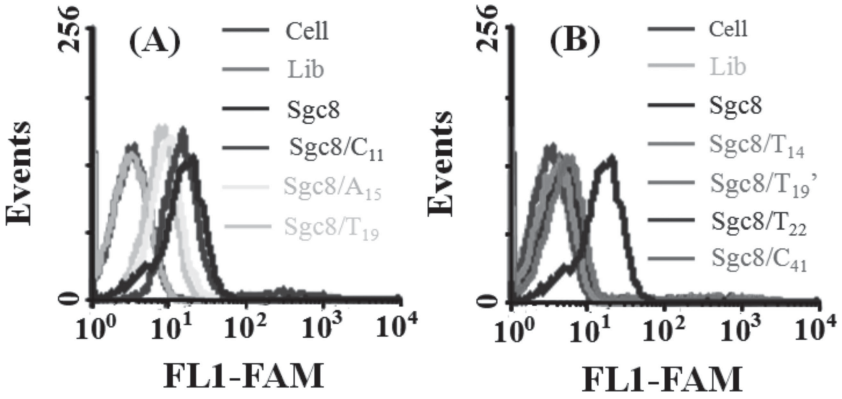

Figure 1. Flow cytometry results of aptamer/cDNA complex binding with CCRF-CEM A) A part and B) B part of Sgc8 complementary sequences. DNA sequences: C41: 5′-TCT AAC CGT ACA GTA TTT TCC CGG CGG CGC AGC AGT TAG AT-3′; A part: C11, 5′-TCT AAC CGT AC-3′ A15, 5′-TCT AAC CGT ACA GTA-3′ T19, 5′-TCT AAC CGT ACA GTA TTT T-3′; B part: T14, 5′-CGC AGC AGT TAG AT-3′ T19′, 5′-GGC GGC GCA GCA GTT AGA T-3′ T22, 5'-CCC GGC GGC GCA GCA GTT AGA T-3′.

2.3. Selection of DNA Sequence as Reporter to Link Photosensitizer

To establish a method for multimodal cancer therapy, a cultured precursor T cell acute lymphoblastic leukemia (ALL) cell line, CCRF-CEM, was used as the model target cell, and a B-cell line from human Burkitt's lymphoma, Ramos, was used as the negative control. Sgc8, an aptamer targeting CCRF-CEM, binds to the target cancer cells with high affinity through the recognition of target membrane protein, human protein tyrosine kinase-7 (PTK7).[13] The Ce6-labeled short DNA sequences hybridize with the Sgc8 aptamer on the AuNR surface, resulting in close proximity of Ce6 to the gold surface and, hence, efficient fluorescence quenching. However, upon aptamer-cell recognition, Ce6 is released to produce singlet oxygen when irradiated. In order to choose an appropriate oligonucleotide as a reporter to link Ce6, we systematically cut the complementary sequences (C_{41}) of Sgc8 into shorter DNA sequences (cDNA) with different lengths: A part, including C_{11}, A_{15} and T_{19} and B part, including T_{14}, T_{19}' and T_{22} (**Figure 1**). Based on mobility variance,[30] polyacrylamide gel electrophoresis (PAGE) (Figure S3, Supporting Information) showed that Sgc8 or C_{41} oligomers, which are single-stranded DNA containing 41 bases, moved faster than any of the Sgc8/cDNA complexes, confirming the successful hybridization of short sequences with Sgc8.

Flow cytometry was used to monitor the binding of dye-modified aptamers with CCRF-CEM and Ramos cells. As expected, the fluorescence signals of all complementary sequences (from C_{11} to C_{41}) were as weak as those of the negative library (Lib), suggesting that these DNA sequences bind neither CEM nor Ramos cells (Figure S4, Supporting Information). Furthermore, Sgc8/cDNA complexes did not bind to negative-control Ramos, thereby preserving target-selectivity and providing a low background (Figure S5, Supporting Information).

In Figure 1, the very strong fluorescence signal shows that Sgc8 effectively targeted CCRF-CEM cells via recognition of PTK7 membrane protein.[13] For this work, a suitable Ce6-reporter should not block the aptamer from binding with target, but it should be released upon binding to produce singlet oxygen. For the A part of Sgc8 complementary sequences, the Sgc8/cDNA complexes exhibited progressively weaker cell-binding with increasing cDNA base numbers. Still, a binding signal could always be observed, suggesting that Sgc8 continues to bind target cancer cells after hybridization with cDNA. The weakened binding between aptamer and target cancer cells was attributed to the competition between cDNA and cells. However, the Sgc8/cDNA complexes in the B part induced an even weaker signals, as monitored by flow cytometry, than the A part. Furthermore, after hybridization with the perfectly complementary C_{41} sequence, Sgc8 had the weakest binding signal, similar to that of the negative control (random library sequences), indicating that the hybridization of Sgc8 with C_{41} completely blocks the binding of aptamer and target cells.

The distinct binding affinity can first be attributed to the A part, which contains more A and T bases that interact more weakly than G and C bases by fewer hydrogen bonds. For example, T_{19} and T_{19}' are both composed of 19 bases. As shown in Figure 1, T_{19} is rich in A and T bases, while T_{19}' is a GC-rich sequence. The data based on software from Integrated DNA Technologies (Table S1, Supporting Information) show that the free energy of Sgc8/T_{19}' is –41.92 kcal mol^{-1}, which is much lower than that of Sgc8/T_{19} (–30.91 kcal mol^{-1}). As a result, the melting temperature of the Sgc8/T_{19}' conjugate is much higher (69.5 °C vs. 56.3 °C), suggesting that Sgc8/T_{19}' is more stable than Sgc8/T_{19}. The short DNA pieces in the stable structure of the Sgc8/cDNA complex are not easily released and are thus unsuitable as a reporter. In previous work,[31] the binding affinity of Sgc8 with CCRF-CEM was studied by conjugating with various

NANO MICRO small

numbers of azobenzene moieties in different positions of oligonucleotide, revealing that the GC-rich portion of the loop is important for cell binding. In this work, when the A part hybridizes with Sgc8, the other part of Sgc8 is still free to bind CCRF-CEM to form the molecular beacon structure, promoting the release of photosensitizer-labeled reporter. For the B part, the stable hybridization complex blocks the binding of Sgc8 with target cells, which reduces the binding affinity of aptamer with target. Furthermore, the duplex of Sgc8-B part is difficult to break upon binding owing to the stable structure with low free energy and high melting temperature. Therefore, the short DNA sequences in the B part are not adaptable as reporters, and we chose the reporter from the A part of Sgc8 complementary sequences.

We further modified Sgc8 with fluorophore FAM and short cDNAs in the A part (C_{11}, A_{15} and T_{19}) with the Dabcyl quencher to determine the hybridization strength between Sgc8 and short sequences. The fluorescence quenching assay (Figure S6A, Supporting Information) proved that the fluorescence of Sgc8 was quenched by short DNA with the quenching efficiency of 72.7%, 91.5% and 94.9%, respectively for C_{11}, A_{15} and T_{19}, which also confirmed the formation of Sgc8/cDNA duplexes. The same sequences were also used to determine the binding between cells and Sgc8/cDNA complexes by flow cytometry. Compared with the library sequence, the increasing intensity of the fluorescence signals in the order of $T_{19}<A_{15}<C_{11}$ (Figure S6B, Supporting Information) suggests that the Dabcyl-labeled cDNA has been released upon target binding. The short C_{11} sequence is not useful as a reporter because the comparatively low quenching efficiency of 72.7% will result in a high background and side effects. On the other hand, the weak binding signal of Sgc8/T_{19} with target cancer cells makes the long T_{19} sequence unsuitable as a reporter as well, even though it has high quenching efficiency. Thus, A_{15} was chosen as the reporter because of the high quenching efficiency of 91.5% and the strong binding signal.

Since Sgc8 is an "always off" aptamer when linked to the gold surface,[32] the cellular binding of Sgc8-NR/cDNA conjugates was confirmed using polyethylene glycol (PEG) as a spacer to avoid the quenching effect of the gold surface.[27,28] The flow cytometry data of the Sgc8-NR conjugate (**Figure 2**) showed stronger cellular binding compared with pure Sgc8 probe because one nanorod can carry multiple aptamers.[27,28] In addition, the Sgc8-NR/cDNA conjugate also produced stronger signals than Sgc8/cDNA. On the contrary, Ramos showed no binding signals, irrespective of the presence of cDNA. Confocal imaging (**Figure 3**) using Sgc8 modified with TAMRA on the 5′-end also confirmed the specific binding. At 4 °C, the TAMRA-modified Sgc8-NR/A_{15} complex displayed very strong fluorescence at the cell surface of CCRF-CEM cells based on the recognition of the target membrane protein PTK7.[13] This result suggests that A_{15} sequence was released from the complex after the specific binding of aptamer with target cells. In comparison, Ramos, the negative control cells, displayed a very weak signal, indicating that the Sgc8-NR/A_{15} did not come close to the Ramos control or were internalized, suggesting that the Sgc8-NR/A_{15} complexes preserved high target selectivity.

2.4. Targeted Cancer Therapy

2.4.1. Photodynamic Therapy

The fluorescence change of Ce6 was verified before and after its linkage to the gold surface. The A_{15}-linked Ce6 fluorescence was quenched after hybridizing with SH-modified Sgc8 on the surface of AuNRs, and the number of aptamers per AuNR was about 70 (Figure S7, Supporting Information). Singlet oxygen sensor green (SOSG), a singlet oxygen-specific indicator, showed that $^1O_2$ generation was quenched by Sgc8-SH modified NRs, but was recovered after binding with CEM (**Figure 4**A). However, for Ramos cells, $^1O_2$ generation did not recover. As shown in Figure 4B, during the 3 h of light irradiation, cell viability of CEM decreased regularly, while Ramos survived, with more than 90% cell viability. These results show that the Ce6-labeled A_{15} reporter was released from the Sgc8-NRs conjugates to dynamically kill the target CEM cells upon light irradiation and avoid harm to nontarget cells.

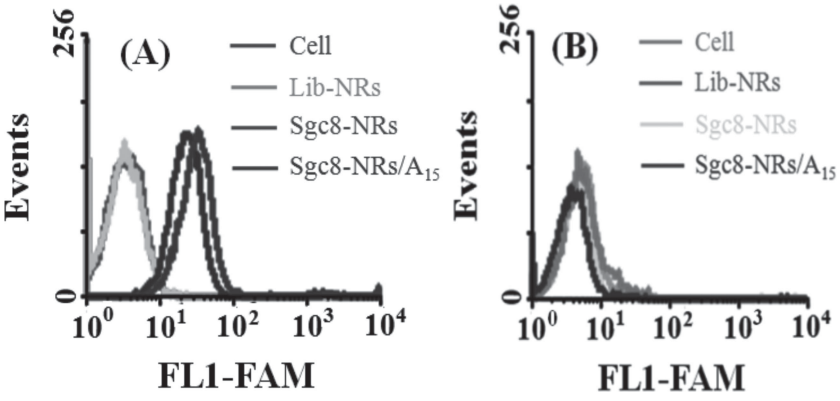

Figure 2. Flow cytometry assay of Sgc8-NRs/A_{15} complex binding with A) CCRF-CEM and B) Ramos.

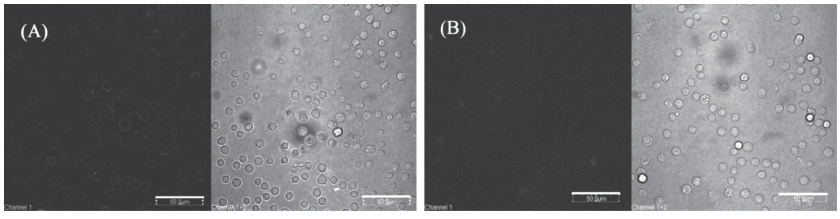

Figure 3. Confocal imaging assay to monitor the fluorescence of TAMRA-modified Sgc8-NRs/A_{15} complex binding with A) CCRF-CEM and B) Ramos. In each picture, the left side is the fluorescence image, and the right side is the overlay of optical and fluorescence images. Scale bar: 50 μm.

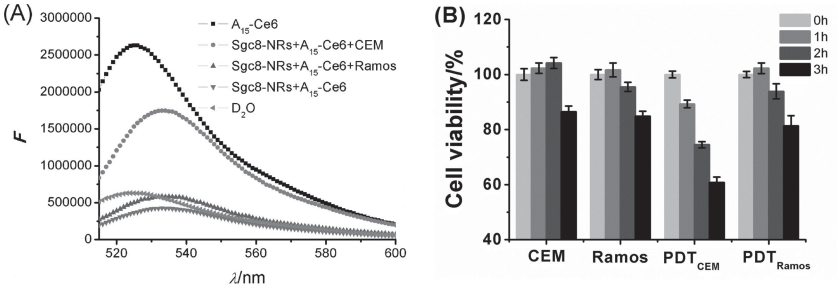

Figure 4. Fluorescence spectra of A) Ce6-labeled A_{15}/Sgc8-NR complex and B) cell viability data of photodynamic therapy under white light irradiation.

There are several reasons why the photosensitizer is released and active only on the target cell surfaces. First, the specificity test (Figure 4) showed that the photodynamic therapy was specific for CEM, due to the binding of PTK7 cell membrane protein with the aptamer,[13] which disrupts the dsDNA structure of aptamer/A_{15}-Ce6 to release Ce6. Since the recognition involves the membrane proteins, it is logical that the released Ce6 remains very near the target cell membrane. The Wilson group designed a peptide-linked activatable photosensitizer Ce6 cleaved by a matrix metalloproteinase-7 for photodynamic therapy,[24] which was very similar to our case. Since the resulting PDT showed high specificity for targeted cancer therapy, it is expected that effective colocalization of the photosensitizer will increase the efficiency and specificity of PDT in our work.

Second, Peng et al.[33] showed that negatively charged hydrophobic photosensitizers such as Ce6 tend to concentrate on the surface of membranes with minimal electrostatic drive to actually traverse them. Therefore, the released Ce6 in our work tends to be on the target cell surface. Furthermore, the binding and irradiation work using Ce6 were carried out at 4 °C, so there should have been no internalization of the membrane-bound conjugates.[34] Thus, the cell membrane is very likely the principal target for Ce6.[35] Third, animal studies[36] found Ce6 to be a useful photosensitizer with low toxicity and preferential tumor localization, which could further reduce nonspecific damage to the normal cells.

Fourth, during photodynamic therapy, the singlet oxygen has a lifetime of several microseconds in aqueous environments[37] and a limited cellular diffusion distance of about 20 nm.[38] In addition, cytotoxic singlet oxygen has a very short radius of action in comparison with the size of tumor cells (>10 μm) and the distance between cells.[37] These physical features will keep the localized concentration of singlet oxygen high on the surface, compared to the surrounding area. Since the number of aptamer-NR conjugates is minimal in our experiments, only those concentrated on cell membrane surface will be effective in targeted therapy.

All of the above reasons suggest that the released Ce6 will perform targeted therapy, as they are most likely concentrated on the target cell surfaces, so that side effects will be minimal as shown in our results.

2.4.2. Photothermal Therapy

Having discussed the effects of PDT, we turn to the photothermal properties of AuNRs, which can transfer light energy into heat.[19] As shown in **Figure 5**A, in the absence of NRs, the temperature was lower than 37 °C after NIR laser irradiation, but it increased to as high as 55 °C in the presence of Sgc8-NR/A_{15}. Because of the binding of Sgc8-NR/A_{15} with CEM, the NIR laser irradiation also enhanced the cell-surface local temperature, leading to cell destruction. Furthermore, Sgc8 binds to target cells at temperatures as high as 55 °C, so there should be no problem with dissociation as the AuNRs are heated (Figure S8A, Supporting Information).[39] However, since Ramos did not bind Sgc8/A_{15}-NRs (Figures 2,3), no NRs were near the cell surface, and the light energy was not converted to heat. The results in Figure 5B indicate that aptamer-NRs conjugates can selectively kill target cancer cells via the PTT effect, thus providing a secondary therapy in addition to the use of PDT.

The melting temperature of the Sgc8/A_{15} conjugate is ca. 51.6 °C, while Sgc8-NRs can increase the environmental temperature to as high as 55 °C after laser irradiation, which can reach the melting temperature of Sgc8/A_{15} (Table S1, Supporting Information). Therefore, it is assumed that the laser-induced temperature enhancement can also promote release of the Ce6-A_{15} sequence at the cell surface,[29] thus providing a secondary, and, perhaps, additive PDT effect presumably because such high temperature accelerates the dehybridization process.[12,29]

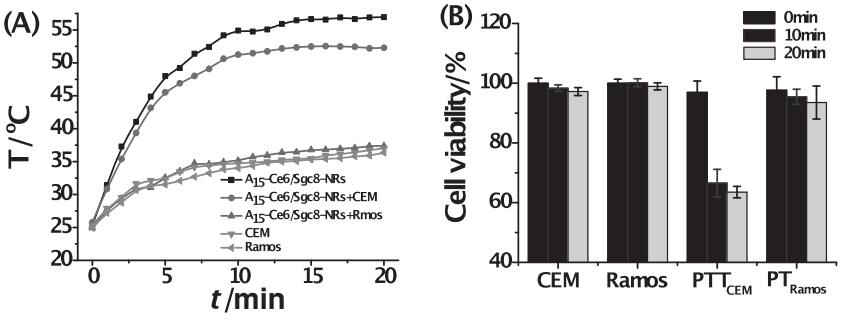

Figure 5. A) Photothermal response of Ce6-labeled A_{15}/Sgc8-NR complex and B) PTT results with laser irradiation.

2.4.3. Combinatorial Multimodal Cancer Therapy

Figure 6 summarizes the therapy data expressed as the mean ± standard deviation and statistical differences assessed by the Student's t test, when all cells were incubated with Ce6-labeled A_{15}/Sgc8-NR conjugates. The control cells without light irradiation showed no damage effect. In photodynamic therapy, white light irradiation led to a decrease in cell viability to around 74.5% ($p<0.05$). After 10 min NIR laser (812 nm) irradiation, the cell viability

NANO MICRO small

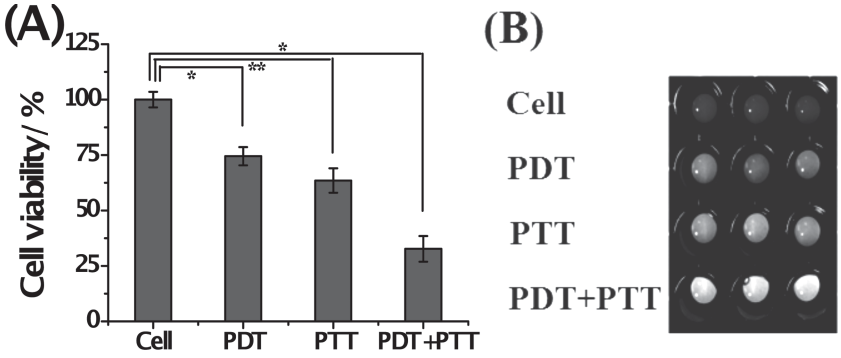

Figure 6. A) Cell viability data and B) imaging of CCRF-CEM cells with PDT, PTT or combinatorial therapy. P values were calculated by the Student's *t* test: *p<0.05, **p<0.001, ***p < 0.0001, n = 3.

decreased to about 63% (p<0.001) due to the photothermal killing of cancer cells. Under both white light and NIR laser irradiation (dualmodal therapy of PDT and PTT), the cell viability was dramatically dropped to below 32% (p<0.05), proving that Ce6-labeled A_{15}/Sgc8-NRs enhanced photodestruction efficiency via multimodal therapy. The control cell assay (Figure S9, Supporting Information) showed that the Ce6-labeled A_{15}/Sgc8-NRs complex were considerably less phototoxic (cell viability is about 90%) to the non-target Ramos cells.

3. Conclusion

In summary, using leukemia as a model cancer for proof of concept, a switchable aptamer-based photosensitizer-AuNR platform for targeted therapeutic activity has been successfully designed for multimodal therapy including both PTT/PDT. This has greatly enhanced the therapeutic effect with high selectivity. In this work, AuNRs are not only useful for photothermal therapy but are also helpful for the delivery and activation of photosensitizer molecules. Because the advantages of aptamers, this method offers highly selective and specific targeting of cancer cells. It is expected that this PDT/PTT strategy has the potential to become a clinically viable and versatile method for targeting and killing cancers.

4. Experimental Section

Preparation of AuNRs: AuNRs were synthesized according to the seed-mediated protocol.[26] First, Au seeds were prepared by reducing 2.5×10^{-4} M $HAuCl_4 \cdot 4H_2O$ with 9.0×10^{-4} M ice-cold $NaBH_4$ in the presence of 7.5×10^{-2} M cetyltrimethylammonium bromide (CTAB). After vigorous stirring, the mixture rapidly developed a light-brown color and was kept for 2 h at 27 °C before synthesis of AuNRs. Second, 0.15 mL 0.01 M $AgNO_3$ and 0.16 mL 0.1 M L-ascorbic acid (L-AA) were added to 25.0 mL growth solution containing $HAuCl_4 \cdot 4H_2O$ (4.0×10^{-4} M) and CTAB (9.5×10^{-2} M). During mixing, the solution immediately became colorless. Finally, 0.11 mL of Au seed solution aged for 2 h was added to the growth solution and stirred vigorously for 20 s with the color gradually turning red. The mixed solution was left undisturbed overnight for further growth to obtain AuNRs with a concentration of about 0.80 nM.

DNA Synthesis: All DNA sequences (Table S2, Supporting Information) were synthesized with an ABI3400 DNA/RNA synthesizer (Applied Biosystems, Foster City, CA) with various 5′-modifiers, including tetramethylrhodamine anhydride (TAMRA), FAM, dabcyl- or amino- groups. For the deprotection procedures, the unlabeled sequences, as well as SH-, FAM and dabcyl- modified DNA oligomers, were deprotected in AMA (ammonium hydroxide/40% aqueous methylamine 1:1) at 65 °C for 20–30 min, but TAMRA-labeled DNAs were deprotected with TAMRA deprotection solution (0.05 M potassium carbonate in methanol) at 65 °C for 3–4 h. Sequences labeled with 5′-amino-modifier were deprotected in ammonium hydroxide at 40 °C for 17 h. Then, the cleaved DNA oligomers were transferred into 15 mL plastic tubes and mixed with 250 µL 3.0 M NaCl and 6.0 mL ethanol, after which the samples were placed into a freezer at –20 °C for precipitation. Following that, the samples were centrifuged at 4000 rpm at 4 °C for 20 minutes, and the precipitated DNA products were dissolved in 400 µL 0.2 M triethylamine acetate (TEAA, Glen Research Corp.) for HPLC purification with a reverse-phase HPLC (ProStar, Varian, Walnut Creek, CA) on a C-18 column. The collected DNA products were dried and detritylated by dissolving and incubating in 200 µL 80% acetic acid for 20 min, then precipitated with 20 µL 3.0 M NaCl and 500 µL ethanol and dried with a vacuum dryer. A Cary Bio-300 UV spectrometer (Varian, Walnut Creek, CA) was used to measure absorbance to quantify the sequences.

Synthesis of Aptamer-Photosensitizer (AP): The aptamer-photosensitizer conjugation was prepared with a 5′-amino-modified aptamer with Ce6.[40] To conjugate with the carboxyl group of Ce6 molecule, the 5′-amino group (Glen Research Corp.) -modified DNA oligomer was cleaved with DMT on the ABI3400 DNA/RNA synthesizer. To improve the coupling efficiency and decrease multiple coupling products, the amount of Ce6 was 10 times that of the DNA product in the coupling reaction. Ten micromole Ce6 was mixed with an equal molar amount of N,N′-dicyclohexylcarbodiimide (DCC, Sigma-Aldrich Inc.) and N-hydroxysuccinimide (NHS, Sigma-Aldrich Inc.) in 500 µL N,N-dimethylformamide (DMF) and aptamer for the activation reaction. The product was then washed with acetonitrile until clear and dried by a vacuum dryer. After deprotection with AMA, the sequence was further purified by reverse-phase HPLC. Finally, the concentrations of all sequences were measured by a Cary Bio-300 UV spectrometer.

Functionalization of AuNRs with Aptamer: The functionalization of AuNRs with thiol-modified aptamers followed a published procedure.[27] Before DNA loading, the thiol-functionalized aptamer (0.1 mM) was deprotected by 0.1 mM tris(2-carboxyethyl) phosphine (TCEP) in 50 mM Tris-HCl (pH 7.5) buffer for 1 h at room temperature. To remove excess CTAB, the as-prepared AuNR solution (10.0 mL) was centrifuged at 14000 rpm for 20 min, and the precipitate was redispersed in water. To stabilize and functionalize, 10.0 mL AuNRs were coated with 200 µL freshly prepared 2.0 mM thiol-terminated methoxy poly(ethylene glycol) (mPEG-SH, MW 5000). The resulting mixture was allowed to sit for 1 h at room temperature, followed by the addition of deprotected

thiol-aptamer. The mixtures were then incubated for 16 h and aged for another 12 h with 0.2 M NaCl. Finally, purification was carried out by centrifugation at 12000 rpm for 5 min.

Supporting Information

Supporting Information is available from the Wiley Online Library or from the author.

Acknowledgements

We are grateful to Dr. Kathryn R. Williams for editing the manuscript and John W. Munson for detecting the temperature curve with a laser sensor. J. W. received the financial support from the China Scholarship Council (CSC) and Southwest University (SWU112092). This work is supported by grants awarded by the National Institutes of Health (GM079359 and CA133086), by the National Key Scientific Program of China (2011CB911000), NSFC (Grant 21221003) and China National Instrumentation Program 2011YQ03012412. We also thank the National Natural Science Foundation of China (No. 21035005), China NSFC (20805038) as well as the China National Grand Program on Key Infectious Disease (2009ZX10004-312), the Key Project of Natural Science Foundation of China (90606003), the International Science & Technology Cooperation Program of China (2010DFB30300).

[1] A. Jemal, R. Siegel, J. Xu, E. Ward, *Ca-Cancer J. Clin.* **2010**, *60*, 277.
[2] M. V. Blagosklonny, *Leukemia* **2006**, *20*, 385.
[3] H. W. Chen, C. D. Medley, K. Sefah, D. Shangguan, Z. Tang, L. Meng, J. E. Smith, W. Tan, *ChemMedChem* **2008**, *3*, 991.
[4] E. C. Dreaden, S. C. Mwakwari, L. A. Austin, M. J. Kieffer, A. K. Oyelere, M. A. El-Sayed, *Small* **2012**, *8*, 2819.
[5] M. K. Yu, D. Kim, I.-H. Lee, J.-S. So, Y. Y. Jeong, S. Jon, *Small* **2011**, *7*, 2241.
[6] R. V. J. Chari, *Acc. Chem. Res.* **2008**, *41*, 98.
[7] R.-M. Kong, X.-B. Zhang, Z. Chen, W. Tan, *Small* **2011**, *7*, 2428.
[8] J. Wang, P. Zhang, J. Y. Li, L. Q. Chen, C. Z. Huang, Y. F. Li, *Analyst* **2010**, *135*, 2826.
[9] J. Zhang, L. Wang, D. Pan, S. Song, F. Y. C. Boey, H. Zhang, C. Fan, *Small* **2008**, *8*, 1196.
[10] L. Q. Chen, S. J. Xiao, P. P. Hu, L. Peng, J. Ma, L. F. Luo, Y. F. Li, C. Z. Huang, *Anal. Chem.* **2012**, *84*, 3099.
[11] S. J. Xiao, P. P. Hu, X. D. Wu, Y. L. Zou, L. Q. Chen, L. Peng, J. Ling, S. J. Zhen, L. Zhan, Y. F. Li, C. Z. Huang, *Anal. Chem.* **2010**, *82*, 9736.
[12] J. Wang, G. Zhu, M. You, E. Song, M. I. Shukoor, K. Zhang, M. O. D. Altman, Y. Chen, Z. Zhu, C. Z. Huang, W. Tan, *ACS Nano* **2012**, *6*, 5070.
[13] D. Shangguan, Y. Li, Z. Tang, Z. C. Cao, H. W. Chen, P. Mallikaratchy, K. Sefah, C. J. Yang, W. Tan, *Proc. Natl. Acad. Sci. USA* **2006**, *103*, 11838.
[14] X. Fang, W. Tan, *Acc. Chem. Res.* **2010**, *43*, 48.
[15] M. Famulok, J. S. Hartig, G. Mayer, *Chem. Rev.* **2007**, *107*, 3715.
[16] J. Wang, P. Zhang, C. M. Li, Y. F. Li, C. Z. Huang, *Biosens. Bioelectron.* **2012**, *34*, 197.
[17] T. S. Hauck, A. A. Ghazani, W. C. W. Chan, *Small* **2008**, *4*, 153.
[18] L. Zhang, H. Chen, J. Wang, Y. F. Li, J. Wang, Y. Sang, S. J. Xiao, L. Zhan, C. Z. Huang, *Small* **2010**, *6*, 2001.
[19] B. Jang, Y. S. Kim, Y. Choi, *Small* **2010**, *7*, 265.
[20] Y.-L. Luo, Y.-S. Shiao, Y.-F. Huang, *ACS Nano* **2011**, *5*, 7796.
[21] B. Jang, J.-Y. Park, C.-H. Tung, I.-H. Kim, Y. Choi, *ACS Nano* **2011**, *5*, 1086.
[22] W.-S. Kuo, C.-N. Chang, Y.-T. Chang, M.-H. Yang, Y.-H. Chien, S.-J. Chen, C.-S. Yeh, *Angew. Chem. Int. Ed.* **2010**, *49*, 2711.
[23] Z. Tang, Z. Zhu, P. Mallikaratchy, R. Yang, K. Sefah, W. Tan, *Chem. Asian J.* **2010**, *5*, 783.
[24] G. Zheng, J. Chen, K. Stefflova, M. Jarvi, H. Li, B. C. Wilson, *Proc. Natl. Acad. Sci. USA* **2007**, *104*, 8989.
[25] D. Shangguan, Z. Tang, P. Mallikaratchy, Z. Xiao, W. Tan, *ChemBioChem* **2007**, *8*, 603.
[26] J. Wang, Y. F. Li, C. Z. Huang, *J. Phys. Chem. C* **2008**, *112*, 11691.
[27] Y.-F. Huang, H.-T. Chang, W. Tan, *Anal. Chem.* **2008**, *80*, 567.
[28] Y.-F. Huang, K. Sefah, S. Bamrungsap, H.-T. Chang, W. Tan, *Langmuir* **2008**, *24*, 11860.
[29] L. Poon, W. Zandberg, D. Hsiao, Z. Erno, D. Sen, B. D. Gates, N. R. Branda, *ACS Nano* **2010**, *4*, 6395.
[30] C. Hong, M. Hagihara, K. Nakatani, *Angew. Chem. Int. Ed.* **2011**, *50*, 4390.
[31] J. A. Phillips, H. Liu, M. B. O'Donoghue, X. Xiong, R. Wang, M. You, K. Sefah, W. Tan, *Bioconjugate Chem.* **2011**, *22*, 282.
[32] H. Shi, X. He, K. Wang, X. Wu, X. Ye, Q. Guo, W. Tan, Z. Qing, X. Yang, B. Zhou, *Proc. Natl. Acad. Sci. USA* **2011**, *108*, 3900.
[33] Q. Peng, J. Moan, J. M. Nesland, *Ultrastruct. Pathol.* **1996**, *20*, 109.
[34] A. R. Oseroff, D. Ohuoha, T. Hasan, J. C. Bommer, M. L. Yarmush, *Proc. Natl. Acad. Sci. USA* **1986**, *83*, 8744.
[35] B. A. Lindig, M. A. J. Rodgers, *Photochem. Photobiol.* **1981**, *33*, 627.
[36] G. A. Kostenich, I. N. Zhuravkin, A. V. Furmanchuk, E. A. Zhavrid, *J. Photoch. Photobio. B* **1993**, *17*, 187.
[37] J. Moan, K. Berg, *Photochem. Photobiol.* **1991**, *53*, 549.
[38] J. D. Spikes, *J. Photoch. Photobio. B* **1990**, *6*, 259.
[39] Z. Xiao, D. Shangguan, Z. Cao, X. Fang, W. Tan, *Chem. Eur. J.* **2008**, *14*, 1769.
[40] Z. Zhu, Z. Tang, J. A. Phillips, R. Yang, H. Wang, W. Tan, *J. Am. Chem. Soc.* **2008**, *130*, 10856.

Received: September 2, 2012
Revised: February 12, 2013
Published online: May 10, 2013

